MDPI

Article

Material Quality Filter Model: Machine Learning Integrated with Expert Experience for Process Optimization

Xuandong Wang [1,2,3], Hao Li [4], Tao Pan [3,4], Hang Su [2,*] and Huimin Meng [1]

1 Institute of Advanced Materials and Technology, University of Science and Technology Beijing, Beijing 100083, China
2 Material Digital R&D Center, China Iron & Steel Research Institute Group, Beijing 100081, China
3 Department of Structural Steel, Central Iron and Steel Research Institute, Beijing 100081, China
4 Beijing MATDAO Technology Co., Ltd., Beijing 100081, China
* Correspondence: hangsu@vip.sina.com

Abstract: In the process of material production, the mismatch between raw material parameters and manufacturing processing parameters may lead to fluctuations in product properties and ultimately to unstable or unqualified product quality. In this paper, we propose the concept of the Quality Filter model for process optimization. The Quality Filter model uses the property prediction model as a surrogate model and integrates expert experience and process window constraints to construct a loss function. When raw material parameters are supplied, the suitable processing parameters can be automatically matched, and the processing fluctuation can be used to hedge the fluctuations in raw material, thus stabilizing the product quality and improving overall product properties. A trial production data set of 128 samples of wind power steel from a steel plant was used to test the model. We selected the ellipsoid discriminant analysis model with a classification accuracy rate of 82.81% as the surrogate model, which gives a highly interpretable visualization result. Finally, the results show that the properties of the samples that underwent the optimized process are improved.

1. Introduction

In the process of material production, the parameters that determine product properties divide into two categories: raw material parameters (such as chemical composition, dimensional tolerance, metallurgical quality, etc.) and processing parameters (such as deformation, heat treatment, welding, etc.). One of the main components of material science research is the study of the correlation between these parameters to discover new materials and optimize existing materials [1].

With material science's continuous development and progress, material composition and manufacturing processes are becoming increasingly complex. Quality control for traditional manufacturing relies on process specifications and inspections: setting qualification thresholds for raw materials, setting process windows for the manufacturing [2], and conducting quality inspections on products [3,4]. Nevertheless, there is a phenomenon that has always plagued the manufacturing industry's quality control: "qualified" raw materials and "qualified" processes still have a certain probability of producing an unqualified product. The so-called "narrow window" control is often applied to solve the problem of product quality fluctuation [5,6], but it is bound to increase production costs. Currently, selection and optimization of processing parameters in production are usually conducted by experts and skilled workers, but with staff turnover and retirement, their expert experience might be lost [7–9]. Therefore, a solution is needed to digitize expert knowledge and experience.

Material data analysis methods based on Machine Learning (ML) have been an important focus of research in recent years and are now receiving more attention [10]. Thanks to

their powerful nonlinear mathematical fitting capability, ML algorithms can build connections between composition, processing parameters, and properties of materials [11–13].

Liu et al., constructed a three-layer artificial neural network (ANN) model to predict the mechanical properties of hot-rolled C–Mn steel [14]. Reddy et al., predicted the mechanical properties of low-alloy steel using an ANN model based on alloy chemical composition and heat-treatment parameters [15]. Xie et al., constructed a deep neural network (DNN) and used chemical composition and rolling processing parameters as the DNN input to predict the mechanical properties of hot-rolled steel sheets. The interpretability of the DNN model was then explored [16]. Jung et al., used a Gaussian process regression method to predict the mechanical properties of dual-phase steels based on microstructural feature parameters [17]. Boto et al., used a variety of machine learning regression algorithms to predict metallurgical quality and product performance based on metallurgical process parameters [18]. The ML algorithms represented by ANN only fit the mathematical relationship between input and output parameters, but the physical meanings of these parameters are not considered. At the same time, although most of the prediction models in reported works achieve good mean absolute/square errors, individual samples still have significant prediction errors [16,19], which may be caused by measurement errors and noise in industrial data. More recently, it has been reported that some deep physical parameters are added to ML models as feature parameters to enhance their predictive capability [20]. Xue et al., added the physical feature parameters representing structure chemistry and bonding to the regression model and obtained an excellent prediction result [21]. Lu et al., added the austenitization temperature (T_γ) as a thermodynamic parameter to feature space, and the model shows better generalization performance than traditional ML methods [22]. Wang et al., developed a theory-guided neural network [23]. Compared to the ordinary DNN, the ML model integrated with expert knowledge and experience has better prediction accuracy and is more tolerant of data noise [24].

The property prediction model was established to assist reverse material design and process optimization. Many works use ML models as surrogate models for predicting properties and apply genetic algorithms (GA) to search the feature parameter space and select composition-process parameter combinations with the most potential [20,25]. Mohanty et al., constructed an ANN model to predict the mechanical properties of cold-rolled IF steel sheets and obtained the parameter optimization range through the GA [26]. Sun et al., established an optimization model combining GA and ANN and obtained the chemical composition of a TC11 titanium alloy with excellent properties [27]. Diao et al., combined the two mutually-exclusive properties of carbon steel to achieve comprehensive performance and used the traversal method to search for sample space to find components and process parameters with the most potential [28]. Yan et al., developed a multi-objective optimization algorithm that can formulate appropriate components and process parameters according to the requirements of customized orders [29]. Liu et al., designed a surrogate model based on convolutional neural networks to predict the mechanical properties of HSLA steel and optimized the process parameters using the firefly algorithm [30]. However, the details of the database and optimization results are not given.

At present, most of the reverse design work is trying to obtain products with better properties, but the quality fluctuation problem in the production process is rarely noticed. Moreover, the optimization process is either manually or purely data-driven, and the property prediction model only determines the optimization results. The valuable expert experience accumulated during production has yet to be effectively utilized. At the same time, due to noise in industrial data and uncertainty in DNNs [31,32], design results may violate physical rules or be unfavorable for production control.

The production of materials is a sequential process, and the raw material parameters appear before the process parameters [33]. However, the current optimization work does not distinguish the two types of parameters. Taking steel production as an example, steel is first cast into ingots and then transported to the rolling mill for rolling. Although its composition is set to a fixed value during design, the composition of the ingot produced

still fluctuates around the set value [29]. In order to ensure product quality, the process parameters should be adjusted according to the fluctuation in the raw material parameters to achieve dynamic control.

Based on the above background, this work proposes a Quality Filter model to solve the quality fluctuation problem caused by the mismatch between raw material parameters and processing parameters in industrial production. The Quality Filter model uses the machine learning algorithm as a surrogate model and integrates expert experience and process range constraints to construct a loss function. When the raw material parameters are supplied, the suitable processing parameters can be automatically matched, and the process fluctuation can be used to hedge the fluctuation in raw material, thus stabilizing the product quality and improving overall product properties.

2. Methods

For all material manufacturing processes, the final properties of the product are determined by the raw material and processing techniques. Taking the production of steel materials as an example, the mechanical properties of steel products are determined by their raw material parameters (including chemical composition and metallurgical quality), as well as rolling, heat treatment, and other processing techniques. The relationship between raw materials (C), process (T), and product property (P) can be described as:

$$P = f(C, T) \tag{1}$$

where f represents the mathematical function relationship between these parameters. Figure 1a shows a traditional manufacturing process in which the mismatch between raw material and processing parameters causes product quality fluctuations, ultimately leading to the unstable and unqualified phenomenon. In this work, a Quality Filter (QF) model was proposed, as shown in Figure 1b. Given a set of raw material parameters, suitable processing parameters for this set can be matched, and process fluctuation can be used to hedge raw material fluctuation to stabilize the final product quality and improve overall product quality.
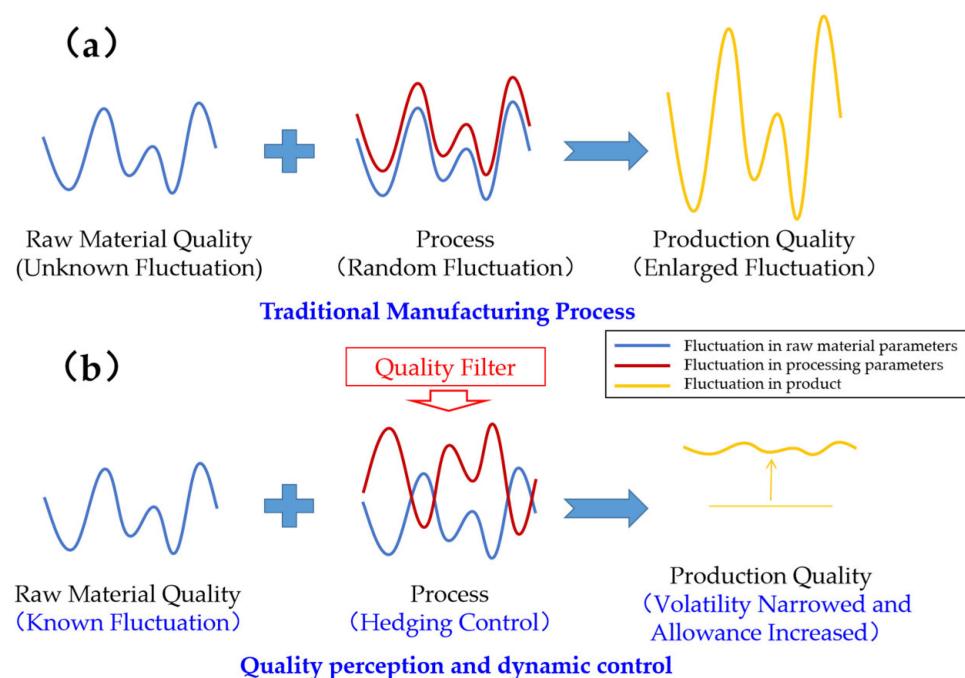

Figure 1. Schematic diagram of the QF model. (**a**) fluctuations in traditional manufacturing process, (**b**) dynamic control through QF model.

2.1. Quality Filter Model

When designing processing parameters in production, material experts usually refer to previous experimental data and make adjustments based on the physical principles of the material. The QF model is also based on this design route, and three factors are considered: the raw-material–process–property prediction model, expert experience, and the process window. The expressions are as follows:

$$\begin{cases} P_i = F_i(C, T) & i = 1, 2, \ldots, L \\ g_j(C, T) = g_j^0 & j = 1, 2, \ldots, m \\ T_k^{mid} = (T_k^{min} + T_k^{max})/2 & k = 1, 2, \ldots, q \end{cases} \tag{2}$$

The first term is the C–T–P prediction model, where F represents its mathematical function and L is the number of concerned product properties. This function can use a variety of machine learning models, including linear regression, neural networks, or other quantitative/semi-quantitative models.

The second term in the formula is the mathematical expression of expert experience, where g represents its mathematical formula and m represents the number of concerned expert experiences. Expert experience refers to empirical rules or conventions that avail production, which implies practical material knowledge. It includes, but is not limited to, the following:

- Known material composition correlation. For example, the sum of all components is 100%, and the sum of several components has the highest limit;
- Known correlation between process parameters, such as the correlation between the processing temperature and the critical temperature of the material's phase transition;
- Other existing theoretical or empirical formulas and expressions.

The digitization of expert experience is represented by mathematical formulas of the above contents and integrated with machine learning models as constraints. The optimization results are required to meet these constraints. For example, in the steel rolling process, the finish rolling temperature T_{FR} is generally about 75 °C above the austenite–ferrite transformation critical temperature T_{Ar3} [34] to ensure the material is in the austenite phase region during the rolling process. This expert experience formula g can be written as $T_{FR} - T_{Ar3} = 75$.

The third term in Equation (2) represents the constraint of the process window, where T_k^{min}, T_k^{max}, and T_k^{mid} are the upper limit, lower limit, and median of the process window, respectively. In practical production, processing parameters use the median to avail manufacture control.

In order to solve for the appropriate process values, an optimization algorithm is needed. Unlike other optimization problems, this work aims not to find the samples with the highest prediction property in the feature space, but to select the sample which can achieve the target property while meeting the expert experience constraints and is closest to the process median. Figure 2 shows the schematic diagram of the optimization process.

According to the C–T–P prediction model, when a target property is chosen, there are usually multiple sets of sample points in the sample space whose prediction property can reach the target. These sample points constitute a potential area. Expert knowledge can be expressed as the mathematical relationship constraints between feature parameters, represented by a hyperplane in the feature space. The part where the potential region intersects with this hyperplane is the sample point set that satisfies both the target property and the expert experience constraint. The sample point closest to the process median in this set is the target optimization point with suitable process parameters.

In order to achieve this optimization process and solve for the suitable process parameters, a loss function can be constructed as follows:

$$\delta = \sum_{i=1}^{L} a_i (f_i(C, T) - P_i)^2 + \sum_{j=1}^{m} b_j (g_j(C, T) - g_j^0)^2 + \sum_{k=1}^{q} c_k (T_k - T_k^{mid})^2 \to 0 \tag{3}$$
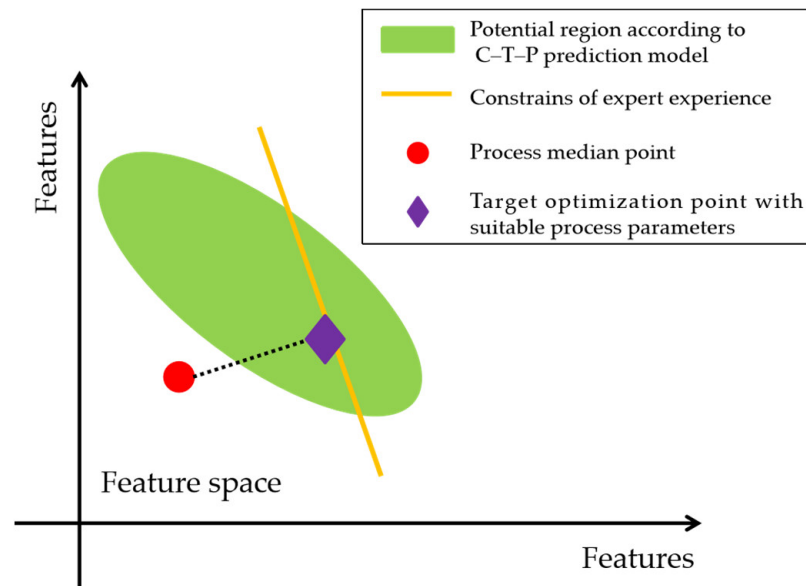
Figure 2. Schematic diagram of the optimization process.

The three items represent the fit degree to the three factors mentioned above, while a_i, b_j, and c_k are the weight value of each factor and default to $a_i = 1$, $b_j = 0.1$, $c_k = 0.01$. The difference in the magnitude of weight values is what allows the C–T–P model to account for the primary influence, and the expert experience constraint accounts for the secondary influence, which ensures that the optimization target point is in the intersection area of these two factors in the sample space. The third weight value usually takes a small value to guarantee a negligible impact on the optimization result, but this simultaneously guarantees that the equation has a unique solution. When the raw material parameters (C) and target properties (P) are set, the processing parameters (T) with the smallest δ value are the optimal result.

2.2. Machine Learning Algorithms

As mentioned above, the C–T–P prediction model accounts for the primary influence on optimization. Therefore, selecting a suitable machine learning model with high precision is very important. Here, we introduce two standard quantitative and semi-quantitative models.

2.2.1. Artificial Neural Network Model

The regression algorithm can establish a mathematical connection between the characteristic parameters and the target value. The trained regression model can predict the target value based on the characteristic parameters. The artificial neural network is a typical regression model inspired by the multi-layered structure and functioning of biological neural systems [35]. Thanks to its strong nonlinear fitting ability, it has been applied to fitting and prediction tasks in material research.

The ANN model has a multi-layer structure. There are one or more hidden layers between the input and output layers, each containing some nodes. Each node has a separate weight, bias, and activation function. For example, the sigmoid function is a commonly used activation function that takes the form:

$$S(x) = 1/\left(1 + e^{-x}\right) \tag{4}$$

The model's training process involves adjusting each node's weights and biases via error back-propagation. However, ANN has a low tolerance for noise in the data and is prone to overfitting.

2.2.2. Discriminant Analysis Model

In order to improve the robustness of the C–T–P model, we also proposed a semi-quantitative Discriminant Analysis (DA) method. By setting the property threshold, the samples were divided into two categories: qualified and unqualified. Then a discriminant function was constructed to separate the two types of samples in high-dimensional sample space.

Usually, discriminant analysis adopts the linear discriminant function. However, in the study of steel and metal, the qualified product can only be obtained when composition and process are well matched within a specific range. Property deterioration may result if these parameters are too high or too low [36,37]. Therefore, the qualified sample region is usually wrapped in the unqualified sample region. In order to describe this characteristic accurately, an "ellipsoid" discriminant function, referring to the literature [38], was adopted, and its form is similar to the standard ellipsoid equation, as follows:

$$F(X_1, X_2, \ldots X_N) \ = \ \sum_{i=1}^{N} (X_i - \overline{X_i})^2 / b_i^2 - 1 \ = \ 0 \tag{5}$$

where $\overline{X_i}$ represents the median of each feature, and b_i is the semiaxis of the "ellipsoid." The purpose of the function is to include the concentratively distributed qualified samples inside the ellipsoid while separating the unqualified samples outside.

Figure 3 shows the training process of the ellipsoid discriminant model. After setting the property thresholds, the data were normalized to eliminate the influence of different orders of magnitude on each parameter. Since the distribution direction of the qualified samples in the hyperspace is usually not parallel to the coordinate axis, principal component analysis (*PCA*) was performed on the qualified data, and all data were transformed according to the *PCA* result, as follows:

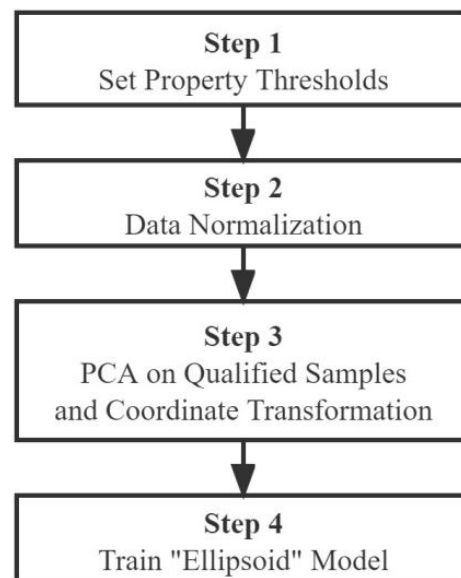$$X \ = \ matrix_{PCA} \times x \tag{6}$$

Figure 3. Training process for the "ellipsoid" discriminant model.

In this paper, x represents the original value of the raw material and processing parameters after normalization. X represents the transformed features used in the model, and $matrix_{PCA}$ is the coordinate transformation matrix based on the *PCA* result of qualified samples. In this way, the concentrated distribution directions of the qualified samples are

parallel to the new coordinate axes, and the "ellipsoid" discriminant function of Equation (5) has the best classification ability.

3. Results and Discussion

The trial production data of 128 samples of wind power steel from a steel plant were studied. The concerned properties of the steel are standard mechanical properties, namely the lower yield strength (R_{eL}) [39] and the impact energy ($AKv_{-20°C}$) [40].

Twelve highly correlative parameters were selected, including seven raw material parameters (chemical element content of C, Mn, S, Nb, and N; steel plate thickness; and blank thickness) and five processing parameters (heating temperature, second-stage rolling temperature, thickness ratio after rough rolling, finish rolling temperature, and after-cooling temperature). Numbers C1–C7 and T1–T5 are used to represent these parameters. Table 1 lists each parameter and property's number, maximum, minimum, mean value, and standard deviation (SD).

Table 1. Wind power steel data set from a steel plant.

Type	No.	Parameter	Min	Max	Mean	SD
Raw Material	C1	C (wt%)	0.15	0.18	0.169	0.0064
	C2	Mn (wt%)	0.93	1.46	1.09	0.1568
	C3	S (wt%)	0.002	0.018	0.008	0.0033
	C4	Nb (wt%)	0.008	0.023	0.011	0.002
	C5	N (ppm)	18	65	37	6.82
	C6	Steel Plate Thickness (mm)	10	60	23	8.9
	C7	Blank Thickness (mm)	220	260	230	17.45
Process	T1	Heating Temperature (°C)	1192	1240	1219	8.7
	T2	Second-Stage Rolling Temperature (°C)	850	1020	938	31.74
	T3	Thickness Ratio After Rough Rolling	1.50	4.15	2.52	0.42
	T4	Finish Rolling Temperature (°C)	785	848	821	11.7
	T5	After-Cooling Temperature (°C)	614	694	657	12.57
Property	P1	R_{eL} (MPa)	358	438	403.1	16.5
	P2	$AKv_{-20°C}$ (J)	112	259	188.6	28.4

It was found that each of the 12 parameters fluctuates within a range and ultimately leads to large-scale fluctuations in the material's properties. As mentioned above, the mathematical relationship between C, T, and P in the QF model can be understood using various quantitative or semi-quantitative models. The C–T–P model has the maximum weight when solving for the process value, so choosing the appropriate model has a significant influence on the filtering result.

3.1. Raw-Material–Process–Property (C–T–P) Model
3.1.1. ANN Model

Firstly, a three-layered back-propagation ANN model with the node number 12–15–1 was used to fit the data. We used the 12 raw materials and processing parameters as input and the P_1 (R_{eL}) value as output and selected the sigmoid function as the activation function. We randomly selected 103 (80%) samples for the training set and used the remaining 25 (20%) to validate the model's generalization ability.

Figure 4a shows the training process for the ANN model. It was found that the Mean Square Error (MSE) of the training set gradually decreased with training, while the MSE of the validation set remained unchanged. This means that overfitting occurred during training, and the model failed to learn the relationship between input and output correctly. Figure 4b,c show the fitting results of the training and validation sets, respectively. The horizontal and vertical coordinates represent the sample property's true value and the model's predicted value. The R-value above represents the distribution slope of the data points. It was found that the R–value of the training set was close to 1, and the true

values of the data points were not much different from the predicted values. However, there is no such feature for the validation set, indicating bad generalization and prediction performance, possibly due to the noise in industrial data or the small amount of data. The network was retrained many times by randomly dividing the data set and changing the network's architecture, but no better result was obtained, which means the quantitative ANN model is unsuitable for this case.
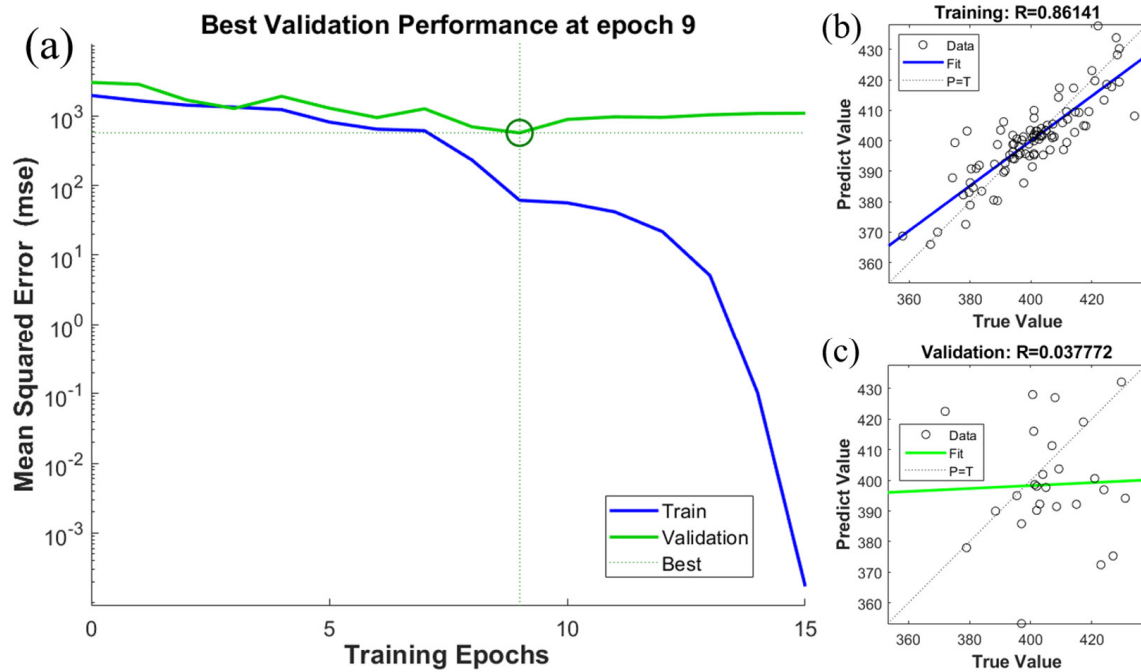

Figure 4. Training and validation results of ANN: (**a**) training process for the ANN model, (**b**) fit result of the training set, (**c**) fit result of the validation set.

3.1.2. Discriminant Analysis Model

The property thresholds were set to $R_{eL} \geq 380$ MPa and $AKv_{-20°C} \geq 190$ J. The data set was divided into 74 qualified and 54 unqualified samples. The discriminant function was constructed according to Equation (5) and trained by the perceptron algorithm. The result of the model shows that there were 22 misclassified samples, and the classification accuracy was 82.81%, which demonstrates that the ellipsoid model effectively expressed the characteristics of the data set. The confusion matrix is shown in Table 2.

Table 2. Confusion matrix of the ellipsoid discriminant model classification result.

Ground Truth Class	Classification Result	
	Qualified	**Unqualified**
Qualified	64	10
Unqualified	12	42

3.1.3. Model Visualization

According to the characteristics of the ellipsoid discriminant function, referring to the literature [38], the N-dimensional sample space was projected to N planes (two-dimensional) through a mapping method for visualization. The horizontal axis of each of the planes is X_i, while the vertical-axis expression is as follows:

$$Y_i = \sum_{j \neq i}^{N} (X_j - \overline{X_j})^2 / b_j^2 \tag{7}$$

Meanwhile, the ellipsoid discriminant analysis function is projected to:

$$F(X_1, X_2, \dots X_N) \ = \ Y_i + (X_i - \overline{X_i})^2 / b_i^2 - 1 \ = \ 0 \tag{8}$$

The two-dimensional projection result of Equation (5) is in parabolic form. Since 12 parameters were selected in this work, 12 visualization results were obtained. Here we take X_{10} as an example, and Figure 5a shows the visualization result. The horizontal and vertical axes can be expressed as:

$$\begin{aligned} X_{10} \ = \ &-3.91C_1 - 0.42C_2 - 7.42C_3 + 62.13C_4 + 0.0023C_5 + 0.0037C_6 + 0.0014C_7 \\ &+8.45 \times 10^{-4}T_1 + 7.71 \times 10^{-4}T_2 - 0.031T_3 - 8.91 \times 10^{-4}T_4 + 5.10 \times 10^{-4}T_5 - 1.06 \end{aligned} \tag{9}$$

$$\begin{aligned} Y_{10} \ = \ &(X_1 - 0.022)^2/4.24 + (X_2 - 0.19)^2/0.77 + (X_3 - 0.31)^2/0.67 + (X_4 - 1.02)^2/0.51 + (X_5 - 0.36)^2/0.43 + \\ &(X_6 - 0.46)^2/0.26 + (X_7 - 0.30)^2/0.22 + (X_8 - 0.23)^2/0.17 + (X_9 + 0.11)^2/0.07 + (X_{11} - 0.32)^2/0.08 + (X_{12} - 0.45)^2/0.029 \end{aligned} \tag{10}$$
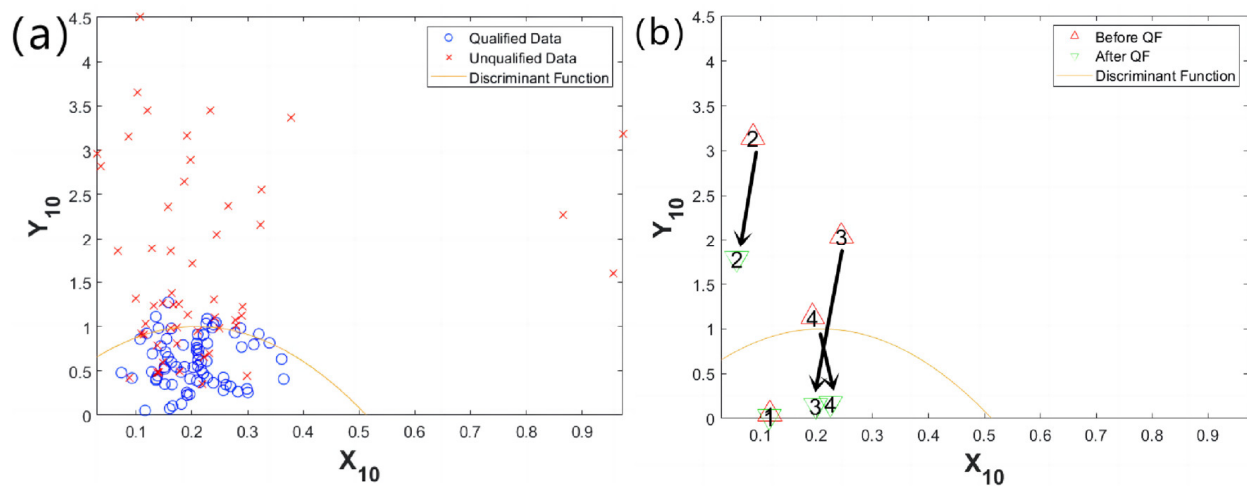

Figure 5. Visualization result of the discriminant analysis model: (**a**) classification result for qualified and unqualified samples, (**b**) comparison results before and after QF, the number represents the sample number.

In Figure 5a, the blue "○" points are qualified samples, the red "×" points are unqualified samples, and the orange parabolic curve is the projected discriminant function that divides the sample space into two regions and correctly separates most of the samples.

3.2. Expert Experience and Process Median

One piece of expert experience was added: the finish rolling temperature T_4 is generally 75 °C above the austenite–ferrite transformation temperature T_{Ar3}, as shown in Equation (11). Table 3 shows the process window and the median of the processing parameters intended to apply.

$$T_4 - T_{Ar3} \ = \ 75 \tag{11}$$

Table 3. Process window and median of processing parameters.

Processing Parameter	Min	Max	Median
T1	1160 (°C)	1250 (°C)	1205 (°C)
T2	850 (°C)	1000 (°C)	925 (°C)
T3	1.5	4	2.75
T4	760 (°C)	860 (°C)	810 (°C)
T5	580 (°C)	720 (°C)	650 (°C)

3.3. Quality Filter Result

After obtaining the three factors and the raw material parameters, the QF model was applied to solve for the suitable processing parameters. The weight factors were $a_i = 1$, $b_j = 0.1$, and $c_k = 0.01$, and the optimization function is shown in Equation (12). In this case, partial differential equations were used to solve for the processing parameters with the smallest δ. In other cases with different C–T–P models, solving for processing parameters may require GA or Bayesian optimization [41].

$$\delta = 1 \times \sum_{i=1}^{12} (X_i - \overline{X_i})^2 / b_i^2 + 0.1 \times (T_3 - T_{Ar3} - 75)^2 + 0.01 \times \sum_{k=1}^{5} (T_k - T_k^{mid})^2 \to 0 \qquad (12)$$

Four samples were selected from the original data set to test the QF model: sample No. 1 was originally a qualified sample, and samples No. 2, 3, and 4 were unqualified. We used the raw material parameters of these samples to solve for new processing parameters via the QF model and compared them with the original samples. Figure 5b shows the comparison results before and after QF. The red "△" points and the green "▽" points represent the position of the samples before and after filtering, respectively. The numbers represent each sample's number, and the same number represents the same raw material parameter. The arrow indicates the position change caused by the change in processing parameters.

It was found that, before filtering, sample No. 1 was located in the "qualified region" and samples No. 2, 3 and 4 were located in the "unqualified region." After filtering, the position of sample No. 1 remained nearly unchanged, while samples No. 2, 3, and 4 moved towards the "qualified region." This indicates that for a certain set of raw material parameters, if there are processing parameters in the data set that make it qualified, the processing parameters given by the model are similar to the original parameters. For unqualified samples, the new processing parameters given by the model will bring the sample inside or as close as possible to the "qualified region," meaning it has the best chance to meet the property threshold. Thus the purpose of filtering is achieved. As for sample No. 2, applying the optimized process parameters still fails to make the sample enter the "qualified region." Table 4 shows the raw material parameters of the four samples. It was found that the C2, C6, and C7 parameters of sample No. 2 deviate from the average value of the data set in Table 1, and the raw material parameters fluctuate more than other samples. Therefore, matching the appropriate process parameters in the set process window is difficult. In production, it is recommended to first adjust the raw material parameters or design a new process window.

Table 4. Raw material parameters and expert experience values of samples No. 3 and No. 4.

	Raw Material Parameters							Expert Experience
Sample No.	C_1	C_2	C_3	C_4	C_5	C_6	C_7	T_{Ar3}
1	0.17	1.02	0.007	0.009	36	24.6	220	\
2	0.17	1.42	0.011	0.010	34	42.5	260	\
3	0.16	1.01	0.007	0.010	30	22.0	220	755 °C
4	0.17	1.00	0.009	0.011	31	20.0	220	750 °C

According to Figure 5b, samples No. 3 and No. 4 have the best filtering results, so validation productions were carried out for these two samples. Tables 4 and 5 compare the product properties with the original processing parameters and new processing parameters given by the model. Expert experience values of samples, represented as T_{Ar3}, were calculated by empirical formula [42].

Table 5. Processing parameters and property comparison before and after Quality Filtering.

Sample No.		Processing Parameters					Property		$R_{eL} \geq 380$ MPa and $Akv_{-20°C} \geq 190$ J
		T_1 (°C)	T_2	T_3 (°C)	T_4 (°C)	T_5 (°C)	R_{eL} (MPa)	$AKv_{-20°C}$ (J)	
3	Original	980	2.55	803	670	1214	369	161	Unqualified
	QF Result	940	2.51	824	664	1220	431	204	Qualified
4	Original	930	2.30	845	660	1231	402	156	Unqualified
	QF Result	953	2.40	819	669	1219	417	187	Nearly Qualified

It was found that for the same raw material, only the hedging adjustment of processing parameters can increase the product's R_{eL} and $Akv_{-20°C}$ by 15–60 MPa and 30–40 J, respectively. Both test samples reached or nearly reached the optimization target of $R_{eL} \geq 380$ MPa and $AKv_{-20°C} \geq 190$ J.

4. Conclusions

This paper proposes a Quality Filter model based on machine learning integrated with expert experience, which can be used to solve the problem of quality fluctuation caused by the mismatch between raw material and processing parameters in material production.

- The model has broad applicability because it can apply various quantitative or semi-quantitative machine learning algorithms.
- It can match appropriate processing parameters according to the fluctuation in raw material parameters to achieve a hedging effect, thereby improving overall product quality and narrowing its property fluctuation.
- A set of trial production data of wind power steel from a steel plant was used to test the model. The results show that for the same raw material, only the hedging adjustment of the processing parameters can increase the product's R_{eL} and $Akv_{-20°C}$ by 15–60 MPa and 30–40 J, respectively. Both test samples reached or nearly reached the optimization target of $R_{eL} \geq 380$ MPa and $AKv_{-20°C} \geq 190$ J.

Author Contributions: Conceptualization, H.S., H.L. and T.P.; programming, X.W.; data resources, H.L. and T.P.; writing—original draft preparation, X.W.; writing—review and editing, H.S. and H.M.; supervision, H.S. All authors have read and agreed to the published version of the manuscript.

Data Availability Statement: The data presented in this study are available on request from the corresponding author. The data are not publicly available due to legal or ethical reasons.

Conflicts of Interest: The authors declare no conflict of interest.

Abbreviations

QF, Quality Filter; ML, Machine Learning; ANN, Artificial Neural Network; DNN, Deep Neural Network; PCA, Principal Components Analysis; MSE, Mean Square Error; C, Raw Material Parameter; T, Processing Parameter; P, Property; C–T–P, Raw-Material–Process–Property.

References

1. Chen, N.; Zhu, D.D.; Wang, W. Intelligent materials processing by hyperspace data mining. *Eng. Appl. Artif. Intell.* **2000**, *13*, 527–532. [CrossRef]
2. De Bussac, A.; Gandin, C.-A. Prediction of a process window for the investment casting of dendritic single crystals. *Mater. Sci. Eng. A* **1997**, *237*, 35–42. [CrossRef]
3. Pernkopf, F. 3D surface acquisition and reconstruction for inspection of raw steel products. *Comput. Ind.* **2005**, *56*, 876–885. [CrossRef]

4. Sun, X.; Gu, J.; Tang, S.; Li, J. Research Progress of Visual Inspection Technology of Steel Products—A Review. *Appl. Sci.* **2018**, *8*, 2195. [CrossRef]
5. Yin, R. *Theory and Methods of Metallurgical Process Integration*; Elsevier: Beijing, China, 2016; pp. 45–49. [CrossRef]
6. Lin, L.; Zeng, J.-Q. Consideration of green intelligent steel processes and narrow window stability control technology on steel quality. *Int. J. Miner. Met. Mater.* **2021**, *28*, 1264–1273. [CrossRef]
7. Sawaragi, T. Human-System Co-Creative Design of Resilience. *IFAC-PapersOnLine* **2016**, *49*, 468–473. [CrossRef]
8. Zarandi, M.F.; Ahmadpour, P. Fuzzy agent-based expert system for steel making process. *Expert Syst. Appl.* **2009**, *36*, 9539–9547. [CrossRef]
9. Merten, D.C.; Hütt, M.-T.; Uygun, Y. A network analysis of decision strategies of human experts in steel manufacturing. *Comput. Ind. Eng.* **2022**, *168*, 108120. [CrossRef]
10. Liu, Y.; Zhao, T.; Ju, W.; Shi, S. Materials discovery and design using machine learning. *J. Mater.* **2017**, *3*, 159–177. [CrossRef]
11. Mandal, S.; Sivaprasad, P.; Venugopal, S.; Murthy, K.; Raj, B. Artificial neural network modeling of composition–process–property correlations in austenitic stainless steels. *Mater. Sci. Eng. A* **2008**, *485*, 571–580. [CrossRef]
12. Liu, S.; Xiong, Z.; Guo, H.; Shang, C.; Misra, R. The significance of multi-step partitioning: Processing-structure-property relationship in governing high strength-high ductility combination in medium-manganese steels. *Acta Mater.* **2017**, *124*, 159–172. [CrossRef]
13. Zhou, Y.; Song, X.; Liang, J.; Shen, Y.; Misra, R. Innovative processing of obtaining nanostructured bainite with high strength—High ductility combination in low-carbon-medium-Mn steel: Process-structure-property relationship. *Mater. Sci. Eng. A* **2018**, *718*, 267–276. [CrossRef]
14. Liu, Z.; Wang, W.-D.; Gao, W. Prediction of the mechanical properties of hot-rolled C Mn steels using artificial neural networks. *J. Mater. Process. Technol.* **1996**, *57*, 332–336. [CrossRef]
15. Reddy, N.S.; Krishnaiah, J.; Hong, S.-G.; Lee, J.S. Modeling medium carbon steels by using artificial neural networks. *Mater. Sci. Eng. A* **2009**, *508*, 93–105. [CrossRef]
16. Xie, Q.; Suvarna, M.; Li, J.; Zhu, X.; Cai, J.; Wang, X. Online prediction of mechanical properties of hot rolled steel plate using machine learning. *Mater. Des.* **2021**, *197*, 109201. [CrossRef]
17. Jung, J.; Yoon, J.I.; Park, H.K.; Kim, J.Y.; Kim, H.S. Bayesian approach in predicting mechanical properties of materials: Application to dual phase steels. *Mater. Sci. Eng. A* **2018**, *743*, 382–390. [CrossRef]
18. Boto, F.; Murua, M.; Gutierrez, T.; Casado, S.; Carrillo, A.; Arteaga, A. Data Driven Performance Prediction in Steel Making. *Metals* **2022**, *12*, 172. [CrossRef]
19. Hwang, R.-C.; Chen, Y.-J.; Huang, H.-C. Artificial intelligent analyzer for mechanical properties of rolled steel bar by using neural networks. *Expert Syst. Appl.* **2010**, *37*, 3136–3139. [CrossRef]
20. Shen, C.; Wang, C.; Wei, X.; Li, Y.; van der Zwaag, S.; Xu, W. Physical metallurgy-guided machine learning and artificial intelligent design of ultrahigh-strength stainless steel. *Acta Mater.* **2019**, *179*, 201–214. [CrossRef]
21. Xue, D.; Balachandran, P.V.; Hogden, J.; Theiler, J.; Xue, D.; Lookman, T. Accelerated search for materials with targeted properties by adaptive design. *Nat. Commun.* **2016**, *7*, 11241. [CrossRef]
22. Lu, Q.; Liu, S.; Li, W.; Jin, X. Combination of thermodynamic knowledge and multilayer feedforward neural networks for accurate prediction of MS temperature in steels. *Mater. Des.* **2020**, *192*, 108696. [CrossRef]
23. Wang, N.; Zhang, D.; Chang, H.; Li, H. Deep learning of subsurface flow via theory-guided neural network. *J. Hydrol.* **2020**, *584*, 124700. [CrossRef]
24. Chen, Y.; Zhang, D. Integration of knowledge and data in machine learning. *arXiv* **2022**, arXiv:2202.10337.
25. Stergiou, K.; Ntakolia, C.; Varytis, P.; Koumoulos, E.; Karlsson, P.; Moustakidis, S. Enhancing property prediction and process optimization in building materials through machine learning: A review. *Comput. Mater. Sci.* **2023**, *220*, 112031. [CrossRef]
26. Mohanty, I.; Bhattacharjee, D.; Datta, S. Designing cold rolled IF steel sheets with optimized tensile properties using ANN and GA. *Comput. Mater. Sci.* **2011**, *50*, 2331–2337. [CrossRef]
27. Sun, Y.; Zeng, W.; Han, Y.; Ma, X.; Zhao, Y. Optimization of chemical composition for TC11 titanium alloy based on artificial neural network and genetic algorithm. *Comput. Mater. Sci.* **2011**, *50*, 1064–1069. [CrossRef]
28. Diao, Y.; Yan, L.; Gao, K. A strategy assisted machine learning to process multi-objective optimization for improving mechanical properties of carbon steels. *J. Mater. Sci. Technol.* **2021**, *109*, 86–93. [CrossRef]
29. Yan, Y.; Lv, Z. A Novel Multi-Objective Process Parameter Interval Optimization Method for Steel Production. *Metals* **2021**, *11*, 1642. [CrossRef]
30. Liu, Y.-C.; Horng, M.-H.; Yang, Y.-Y.; Hsu, J.-H.; Chen, Y.-T.; Hung, Y.-C.; Sun, Y.-N.; Tsai, Y.-H. The Steelmaking Process Parameter Optimization with a Surrogate Model Based on Convolutional Neural Networks and the Firefly Algorithm. *Appl. Sci.* **2021**, *11*, 4857. [CrossRef]
31. Gawlikowski, J.; Tassi, C.R.N.; Ali, M.; Lee, J.; Humt, M.; Feng, J.; Kruspe, A.; Triebel, R.; Jung, P.; Roscher, R.; et al. A survey of uncertainty in deep neural networks. *arXiv* **2022**, arXiv:2107.03342.
32. Laha, D.; Ren, Y.; Suganthan, P. Modeling of steelmaking process with effective machine learning techniques. *Expert Syst. Appl.* **2015**, *42*, 4687–4696. [CrossRef]
33. Backman, J.; Kyllönen, V.; Helaakoski, H. Methods and Tools of Improving Steel Manufacturing Processes: Current State and Future Methods. *IFAC-PapersOnLine* **2019**, *52*, 1174–1179. [CrossRef]

34. Jahazi, M.; Egbali, B. The influence of hot rolling parameters on the microstructure and mechanical properties of an ultra-high strength steel. *J. Mater. Process. Technol.* **2000**, *103*, 276–279. [CrossRef]

35. Rumelhart, D.E.; Hinton, G.E.; Williams, R.J. Learning representations by back-propagating errors. *Nature* **1986**, *323*, 533–536. [CrossRef]

36. Li, Z.; Chai, F.; Yang, L.; Luo, X.; Yang, C. Mechanical properties and nanoparticles precipitation behavior of multi-component ultra high strength steel. *Mater. Des.* **2020**, *191*, 108637. [CrossRef]

37. Hou, C.; Shan, Y.; Wu, H.; Bi, X. Effect of a small addition of Cr on soft magnetic and mechanical properties of Fe–49Co–2V alloy. *J. Alloys Compd.* **2013**, *556*, 51–55. [CrossRef]

38. Su, H.; Che, Z.-H.; Wu, J.-M.; Li, R. Classification Mapping and Its Application on Chemical Systems. *J. Chem. Inf. Comput. Sci.* **1999**, *39*, 718–727. [CrossRef]

39. Hearn, E. *Mechanics of Materials*; Elsevier: Amsterdam, The Netherlands; University of Warwick: Coventry, UK, 1997; pp. 4–5. [CrossRef]

40. Hashemi, S.; Mohammadyani, D. Characterisation of weldment hardness, impact energy and microstructure in API X65 steel. *Int. J. Press. Vessel. Pip.* **2012**, *98*, 8–15. [CrossRef]

41. Snoek, J.; Larochelle, H.; Adams, R.P. Practical Bayesian Optimization of Machine Learning Algorithms. *arXiv* **2012**, arXiv:1206.2944.

42. Gorni, A. *Steel Forming and Heat Treating Handbook*; Antonio Augusto Gorni: São Vicente, SP, Brazi, 2019; pp. 26–43. [CrossRef]